

WANG Meng, ZHANG Yu, LIANG Chang-hong

Analysis of airborne antenna using a FEM–UTD hybrid method

© Higher Education Press and Springer-Verlag 2006

Abstract In this paper, the near-field vector components were used to combine the FEM method and the uniform-geometrical theory of diffraction (UTD) method for analyzing phased array antenna mounted on an airborne platform. First, HFSS, a set of software based on finite element method (FEM), was utilized to find the near-field vector components of the phased array antennas, and then these vector components were used as the source of the UTD method to get the disturbed radiation pattern. Numerical results show that the hybrid of the two methods not only extends the use of the UTD program, but also effectively solves this type of challenging problems.

Keywords: FEM, UTD, Airborne phased array antenna pattern

1 Introduction

Electromagnetic compatibility (EMC) is very important especially for the aircraft, which is crowded with electronic equipment. The analysis of the airborne phased array is very important. However, because the frequency of the phased array antenna is very high and the airplane is very large, it is difficult to use MOM or FEM method to analyze airborne phased array in such a large system. For this electrically large object, UTD is suitable for predicting the effect of the object when it cannot analyze the characteristic of the antenna itself [1-2].

On the other hand, the antenna is far away from the platform (10λ), so the antenna's character can be analyzed with HFSS without considering the whole airplane. The

antenna's near-field vector component can be computed with HFSS, and then the result is entered into the UTD program to compute the far-field. This is the hybrid method of FEM and UTD. This method works well here because the antenna is far away from the airplane.

2 Vector field component of the antenna

Phased array antenna is a combination of antennas in which there is a control of the phase and power of the signal applied at each antenna, which results in a wide variety of possible radiation patterns (Fig. 1).

ANSOFT HFSS is a software based on the FEM and is widely used in electromagnetic computation field. In fact, the method of FEM blending UTD is that using HFSS to compute the near-field vector component of the antenna first, and then using the UTD method to deal with the effect of the object. This method is suitable here because the antenna is placed 5.4 m away from the plane, and the antenna works in the L-band. This allows us to ignore the effect of the plane when using HFSS to analyze the antenna. The near field vector component is the interface between FEM (HFSS) and UTD.

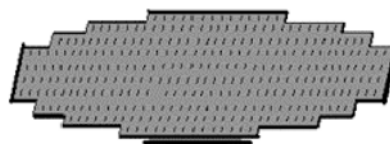


Fig. 1 A phased array antenna

Translated from *Chinese Journal of Radio Science*, 2005, 20(3): 395-399(in Chinese)

WANG Meng(✉), ZHANG Yu, LIANG Chang-hong
National key Laboratory of Antennas and Microwave Technology,
Xidian University, xi'an 710071, China
E-mail: wangm@mail.xidian.edu.cn

3 The analysis of the effect of the object with UTD

The next step is to use UTD to deal with the vector field component simulated with ANSOFT HFSS. The airplane can be simplified as the model made up of a flat plate, cylinder and cone (Fig. 2).



Fig. 2 The model of the airplane

If the reflected or diffracted ray on the flat plate, the cylinder and the cone can be established, the effect on the pattern of the object can be evaluated easily [3]. In this paper, the author uses the reflection of the cylinder as an example.

The first step is ray trace (Fig. 3). The source point and the field point are known, so the objective is to find out the point of reflection θ_r , according to Fermat's theorem.

An infinite length cylinder with radius a is shown in Fig. 3. Point D and E represent the mapping of the source point and the field point to the xoy plane respectively.

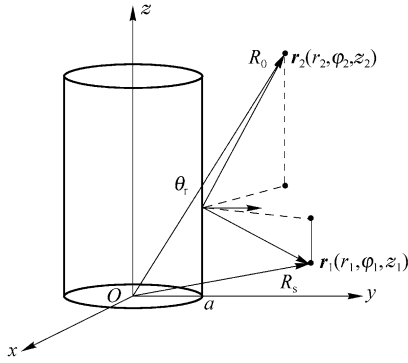


Fig. 3 The ray trace of a cylinder

The source point and field point can be respectively presented as:

$$OR_s: \mathbf{r}_1 = r_1 \cos \varphi_1 \hat{\mathbf{a}}_x + r_1 \sin \varphi_1 \hat{\mathbf{a}}_y + z_1 \hat{\mathbf{a}}_z \quad (1)$$

$$OR_0: \mathbf{r}_2 = r_2 \cos \varphi_2 \hat{\mathbf{a}}_x + r_2 \sin \varphi_2 \hat{\mathbf{a}}_y + z_2 \hat{\mathbf{a}}_z$$

Assume the reflected point θ_r existed, then;

$$\overline{O\theta_r} = a \cos \varphi \hat{\mathbf{a}}_x + a \sin \varphi \hat{\mathbf{a}}_y + z \hat{\mathbf{a}}_z \quad (2)$$

$$\overline{\theta_r R_s} = (r_1 \cos \varphi_1 - a \cos \varphi) \mathbf{a}_x + (r_1 \sin \varphi_1 - a \sin \varphi) \mathbf{a}_y + (z_1 - z) \mathbf{a}_z$$

$$\overline{\theta_r R_0} = (r_2 \cos \varphi_2 - a \cos \varphi) \mathbf{a}_x + (r_2 \sin \varphi_2 - a \sin \varphi) \mathbf{a}_y + (z_2 - z) \mathbf{a}_z \quad (3)$$

Note that the outward normal vector \mathbf{n} is independent of the z direction, and we get:

$$\hat{\mathbf{n}} = \cos \varphi \mathbf{a}_x + \sin \varphi \mathbf{a}_y \quad (4)$$

According to Fermat's theorem, the incident angle is equal to the reflected angle, then:

$$\frac{\overline{\theta_r R_s} \cdot \hat{\mathbf{n}}}{|\overline{\theta_r R_s}|} = \frac{\overline{\theta_r R_0} \cdot \hat{\mathbf{n}}}{|\overline{\theta_r R_0}|} \quad (5)$$

$$\frac{r_1 \cos(\varphi - \varphi_1) - a}{|\overline{\theta_r R_s}|} = \frac{r_2 \cos(\varphi - \varphi_2) - a}{|\overline{\theta_r R_0}|} \quad (6)$$

Let $\theta_1 = \varphi - \varphi_1$ $\theta_2 = \varphi_2 - \varphi$, then Eq. (6) can be deduced to:

$$\frac{r_1 \cos \theta_1 - a}{|\overline{\theta_r R_s}|} = \frac{r_2 \cos \theta_2 - a}{|\overline{\theta_r R_0}|} \quad (7)$$

Here, L is the total optical distance, i.e.,

$$L = |\overline{\theta_r R_s}| + |\overline{\theta_r R_0}| \quad (8)$$

$$\begin{cases} |\overline{\theta_r R_s}| = \sqrt{r_1^2 + a^2 - 2ar_1 \cos \theta_1 + (z_1 - z)^2} \\ |\overline{\theta_r R_0}| = \sqrt{r_2^2 + a^2 - 2ar_2 \cos \theta_2 + (z_2 - z)^2} \end{cases} \quad (9)$$

According to Fermat's theorem, we get:

$$\begin{cases} \frac{\partial L}{\partial \varphi} = \frac{ar_1 \sin \theta_1}{|\overline{\theta_r R_s}|} - \frac{ar_2 \sin \theta_2}{|\overline{\theta_r R_0}|} = 0 \\ \frac{\partial L}{\partial z} = \frac{(z - z_1)}{|\overline{\theta_r R_s}|} - \frac{(z_2 - z)}{|\overline{\theta_r R_0}|} = 0 \end{cases} \quad (10)$$

i.e.,

$$\begin{cases} \frac{r_1 \sin \theta_1}{|\overline{\theta_r R_s}|} = \frac{r_2 \sin \theta_2}{|\overline{\theta_r R_0}|} \\ \frac{(z - z_1)}{|\overline{\theta_r R_s}|} = \frac{(z_2 - z)}{|\overline{\theta_r R_0}|} \end{cases} \quad (11)$$

As is shown in Fig.3, $|\overline{CD}|$ and $|\overline{CE}|$ denote the horizontal projection of $|\overline{CA}|$ and $|\overline{CB}|$ on the plane parallel to the bottom of the cylinder respectively, and therefore we have:

$$\begin{cases} |\overline{\theta_r D}| = \sqrt{|\overline{\theta_r R_s}|^2 - (z - z_1)^2} = \sqrt{a^2 + r_1^2 - 2ar_1 \cos \theta_1} \\ |\overline{\theta_r E}| = \sqrt{|\overline{\theta_r R_0}|^2 - (z_2 - z)^2} = \sqrt{a^2 + r_2^2 - 2ar_2 \cos \theta_2} \end{cases} \quad (12)$$

According to the principle on similar triangle, we get:

$$\frac{(z - z_1)}{|\overline{\theta_r D}|} = \frac{(z_2 - z)}{|\overline{\theta_r E}|} \quad (13)$$

In the following, we normalize the variable:

$$\bar{r}_1 = \frac{r_1}{a} \quad \bar{r}_2 = \frac{r_2}{a} \quad \bar{z} = \frac{z}{a} \quad \bar{z}_1 = \frac{z_1}{a} \quad \bar{z}_2 = \frac{z_2}{a} \quad (14)$$

$$\frac{\bar{r}_1 \cos \theta_1 - 1}{\bar{r}_1 \sin \theta_1} = \frac{\bar{r}_2 \cos \theta_2 - 1}{\bar{r}_2 \sin \theta_2} \quad (15)$$

Equation (15) can be simplified to:

$$\bar{r}_1 \sin \theta_1 - \bar{r}_2 \sin \theta_2 = \bar{r}_1 \bar{r}_2 \sin(\theta_1 - \theta_2) \quad (16)$$

Then, Eq. (16) can be rewritten as:

$$\bar{r}_1 \sin \theta_1 - \bar{r}_2 \sin[(\varphi_2 - \varphi_1) - \theta_1] = \bar{r}_1 \bar{r}_2 \sin[2\theta_1 - (\varphi_2 - \varphi_1)] \quad (17)$$

For the reason of $\theta_2 = (\varphi_2 - \varphi_1) - \theta_1$, it can be simplified as:

$$\begin{aligned} & [\bar{r}_1 + \bar{r}_2 \cos(\varphi_2 - \varphi_1) - 2\bar{r}_1\bar{r}_2 \cos(\varphi_2 - \varphi_1) \cos \theta_1] \sin \theta_1 \\ &= \bar{r}_2 \sin(\varphi_2 - \varphi_1) \cos \theta_1 - 2\bar{r}_1\bar{r}_2 \sin(\varphi_2 - \varphi_1) \cdot \\ & \quad \cos^2 \theta_1 + \bar{r}_1\bar{r}_2 \sin(\varphi_2 - \varphi_1) \end{aligned}$$

Let $x = \cos \theta_1$, then $\sin \theta_1 = \sqrt{1 - x^2}$.

We get:

$$\begin{aligned} & [\bar{r}_1 + \bar{r}_2 \cos(\varphi_2 - \varphi_1) - 2\bar{r}_1\bar{r}_2 \cos(\varphi_2 - \varphi_1)x]^2 (1 - x^2) \\ &= [\bar{r}_2 \sin(\varphi_2 - \varphi_1)x - 2\bar{r}_1\bar{r}_2 \sin(\varphi_2 - \varphi_1)x^2 \\ & \quad + \bar{r}_1\bar{r}_2 \sin(\varphi_2 - \varphi_1)]^2 \end{aligned}$$

Then, the result can be expressed finally as:

$$\begin{aligned} & 4\bar{r}_1^2\bar{r}_2^2x^4 - 4\bar{r}_1\bar{r}_2[\bar{r}_1 \cos(\varphi_2 - \varphi_1) + \bar{r}_2]x^3 \\ & + [\bar{r}_1^2 + \bar{r}_2^2 + 2\bar{r}_1\bar{r}_2 \cos(\varphi_2 - \varphi_1) - 4\bar{r}_1^2\bar{r}_2^2]x^2 \\ & + 2\bar{r}_1\bar{r}_2[2\bar{r}_1 \cos(\varphi_2 - \varphi_1) + \bar{r}_2 + \bar{r}_2 \cos^2(\varphi_2 - \varphi_1)]x \\ & + \{\bar{r}_1^2\bar{r}_2^2 \sin^2(\varphi_2 - \varphi_1) - [\bar{r}_1 + \bar{r}_2 \cos(\varphi_2 - \varphi_1)]^2\} = 0 \end{aligned}$$

From the function above, θ_1 can be solved. Once θ_1 is known, φ , θ_2 can be obtained. Z component of the reflection point can be found out by Eq. (18) as follows:

$$\begin{aligned} \bar{z} &= \frac{\bar{z}_1 |\bar{\theta}_1 \bar{E}| + \bar{z}_2 |\bar{\theta}_1 \bar{D}|}{|\bar{\theta}_1 \bar{E}| + |\bar{\theta}_1 \bar{D}|} \\ &= \frac{\bar{z}_1 \sqrt{1 + \bar{r}_2^2 - 2\bar{r}_2 \cos \theta_2} + \bar{z}_2 \sqrt{1 + \bar{r}_1^2 - 2\bar{r}_1 \cos \theta_1}}{\sqrt{1 + \bar{r}_2^2 - 2\bar{r}_2 \cos \theta_2} + \sqrt{1 + \bar{r}_1^2 - 2\bar{r}_1 \cos \theta_1}} \quad (18) \end{aligned}$$

In summary, Eqs. (17)-(18) form the analytical equations for the reflection point on the cylinder.

This completes the first step. The second step is to judge whether the ray is blocked. The ray is valid only when it is not blocked.

The third step is to compute the electric field at the field point R_0 (Fig. 4).

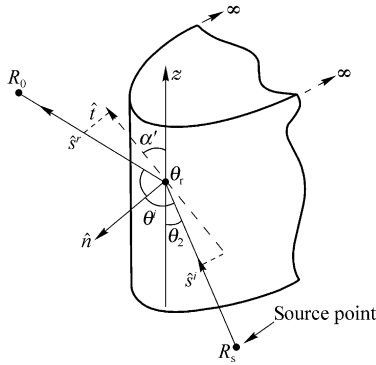


Fig. 4 Reflected field by the cylinder surface.

The reflected field by the cylinder surface can be expressed as follows:

$$\bar{E}^r(R_0) = \bar{E}^i(\theta_r) \bar{R} \sqrt{\frac{\rho_1^r \rho_2^r}{(\rho_1^r + s^r)(\rho_2^r + s^r)}} e^{-jk s^r} \quad (19)$$

The function above is a vector expression. The scalar expression is:

$$\begin{aligned} E^r(R_0) &= C_0 \frac{e^{-jk s^r}}{s^i} \left[-\sqrt{\frac{-4}{\xi^L}} e^{-j(\xi^L)^2/12} \cdot \right. \\ & \quad \left. \left\{ \frac{e^{-j(\pi/4)}}{2\sqrt{\pi \xi^L}} [1 - F(X^L)] + \hat{P}_{s,h}(\xi^L) \right\} \right] \\ & \quad \sqrt{\frac{\rho_1^r \rho_2^r}{(\rho_1^r + s^r)(\rho_2^r + s^r)}} e^{-jk s^r} \quad (20) \end{aligned}$$

The component is detailed in Ref. [4], so we do not present each variable here. Using the formula above, the reflected field by the cylinder surface can be easily computed. The near vector field simulated by HFSS is used as the incident field \bar{E}^i in Eq. (19).

The example above is only the computation of the reflection field by the cylinder surface. Since the airplane is made up of the plate, cylinder and cone, the total UTD program should include these three modules. Furthermore, the other two modules are required to improve the accuracy.

4 Numerical results and discussion

We used an airborne antenna that is 5.4 m away from the airplane, with the antenna working in the L-band. Fig. 5 shows the near-field pattern computed by ANSOFT HFSS. Fig. 6 shows the far-field pattern. The near-field pattern has not been affected by the airplane, as shown in Fig. 5; and the far-field pattern is affected by the airplane obviously.

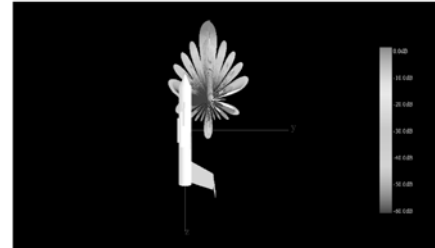


Fig. 5 Near field pattern.



Fig. 6 Far field pattern.

5 Conclusions

To analyze the phased array antenna, the software HFSS based on FEM is a good choice. For an electrically large

target, UTD works well. Combining FEM (HFSS) and UTD is a good method for analyzing the airborne phased array antenna as shown in this paper.

References

1. Wang M.-G., Geometric theory of diffraction, Xi'an: Xidan University publication, 1994
2. Zhang Y., Liang C.-H., Parallel UTD algorithm and its application to the analysis of airborne antennas, *Acta Electronica Sinica*, 2003, 31(3): 332–334
3. Xiang T.-M., Cao X.-Y., Ma F.-G., et al, Analysis of the airborne phased array pattern, *Chinese Journal of Radio Science*, 2002, 17(2): 204–207
4. Pathak P. H., Burnside W. D., Marhefka R. J., A uniform GTD analysis of the diffraction of electro-magnetic waves by a smooth convex surface, *IEEE Trans.*, 1980, AP-28(5): 631–642